

## ELECTRONIC SUPPLEMENTARY MATERIAL

### Simulation of carbon cycling, including dissolved organic carbon transport, in forest soil locally enriched with $^{14}\text{C}$

Journal: Biogeochemistry

E. Tipping, P.M. Chamberlain, Centre for Ecology and Hydrology, Lancaster Environment Centre, Lancaster, LA1 4AP, United Kingdom

M. Fröberg, Department of Soil and Environment, SLU - Sveriges Lantbruksuniversitet, P.O. Box 7001, SE-75007 Uppsala, Sweden.

P.J. Hanson, Environmental Sciences Division, Oak Ridge National Laboratory, Tennessee 37831-6422, USA

P.M. Jardine, Biosystems Engineering and Soil Science Department, University of Tennessee, Knoxville, Tennessee 37996-4531, USA

Corresponding author e-mail [et@ceh.ac.uk](mailto:et@ceh.ac.uk)

## TREE MODEL

The tree carbon model was driven by atmospheric  $^{14}\text{C}$  values at west and east ORR. For the period 1900 to 1995, measured values for the northern hemisphere were used (Reimer et al. 2004; Hua & Barbetti 2004; Levin & Kromer 2004), including dilution due to the Suess effect and enrichment due to weapons testing in the mid-20<sup>th</sup> century. The west of ORR received a number of small  $^{14}\text{C}$  pulses during the growing seasons in 1996, 1997 and 1998, and for those years the atmospheric  $^{14}\text{C}$  content was set to the average tree ring cellulose value in each year (118, 125 and 127 % respectively). For the east, northern hemisphere average values were used during these years. The magnitudes of the 1999  $^{14}\text{C}$  pulses are not known, and are derived from the model. The timing and length of the 1999 pulses were assumed to be the same at both east and west ORR. In order to capture this short-term input, the model, while operating on an annual timestep for other years, was modified to accommodate 7 discrete monthly periods (April to October) in 1999, with the pulse occurring over a one-month period in June.

Net photosynthesis increases during the spring and reaches a maximum at or shortly after full leaf expansion (Larson & Gordon 1969; Reich et al. 1991), whilst newly fixed C is used in leaf growth until leaf maturity, after which all photosynthate not required for in-situ respiration and cellular maintenance is either converted to storage compounds or translocated from the leaf to other parts of the tree (Dickson & Larson 1981). For 1999, the model approximates these processes by constraining the production of leaf material to occur between April and

June, with C in leaf growth in this period derived equally from new C in photosynthate and stored C (Dickson et al. 2000a,b). After June, a small amount of C (5 g) is input into the leaves each month for cellular maintenance, and all other new photosynthate is routed into the tree C store and new root growth. The amount of leaf C derived from leaf growth in June 1999 is found by model fitting, the remainder of leaf growth assumed to occur equally in April and May.

The 10 adjustable parameters, specific to ORR, are listed in Table 2. The first seven refer to the steady-state conditions in the forest, while the last three describe the circumstances during the  $^{14}\text{C}$  pulse of 1999. For each year, the model calculates, by mass balance, the  $^{14}\text{C}$  content of the litterfall and of the roots < 2 mm diameter in the O-horizon and the 0-15 and 15-60 cm soil depths. In order to fit the model, the calculated  $^{14}\text{C}$  values were compared, through squared residuals using the Solver function of Microsoft Excel, with 28 measurements made by Joslin et al. (2006). We combined data for roots of diameter <0.5 mm and 0.5-2 mm to obtain single values for roots <2 mm. Because data for roots at 15-30 cm soil depth were lacking, we used average values for 0-15 and 30-60 cm (which were within 2% modern of each other). The total annual fine root turnover was constrained to be  $105 \text{ g C m}^{-2} \text{ yr}^{-1}$ , estimated for Walker Branch (Hanson et al 2003), and the average root turnover rates were constrained to the measured values of 0.26, 0.13 and  $0.11 \text{ a}^{-1}$ , respectively in O, A and B (Joslin et al. 2006).

Figure S1 shows that the observed  $^{14}\text{C}$  data are reproduced satisfactorily by the optimised parameter values of Table S1. The estimated magnitude of the June 1999  $^{14}\text{C}$  pulse at west ORR, 1470% modern, is large, but not unreasonable given the enrichments observed in tree ring cellulose (up to 270 and 300% modern in 1999 and 2000, respectively), which is built from a mix of new photosynthate-C and stored C, the latter of which contained very little above-background  $^{14}\text{C}$  prior to the 1999 pulse. It is possible that the pulse actually occurred over a shorter period than the assumed one month, in which case the model will underestimate the maximum magnitude of the pulse, but the total amount of  $^{14}\text{C}$  which was assimilated by the trees during the pulse will be the same. Our estimate of the magnitude of the  $^{14}\text{C}$  pulse in east ORR (ca. 300% modern) agrees with that of Gaudinski et al (2009), but for west ORR we estimate a much greater pulse, 1470% modern compared to the Gaudinski et al. (2009) value of 311% modern. The discrepancy arises from the use of different assumptions. Gaudinski et al. (2009) assumed that the pulse at west ORR was of the same magnitude as the  $^{14}\text{C}$  content of west ORR litterfall in 2000, which led them to estimate similar magnitudes for both east and west ORR, while here we did not set the magnitude of the pulse, and let the model find values which best fitted all the data for both west and east ORR. The magnitude of the pulse at west ORR is likely to have been significantly greater

than at east ORR since the  $^{14}\text{C}$  content of litterfall in 2000 was much greater in west ORR (197% modern) than in east ORR (122% modern).

Table S1 Fitted model parameters for vegetation carbon pools.

Parameter	Fitted value
Tree store of C for leaf and root formation ( $\text{g m}^{-2}$ )	278
Fraction of roots with fast turnover	O 0.214 A 0.076 B 0.053
Root turnover rate ( $\text{a}^{-1}$ )	fast 5.95 slow 0.059
Fraction of root C supplied by C storage pools	0.484
Photosynthetic C input to leaves, June 1999 ( $\text{g m}^{-2}$ )	18.2
Atmospheric $^{14}\text{C}$ June 1999 (% modern)	west 1470.2 east 377.8

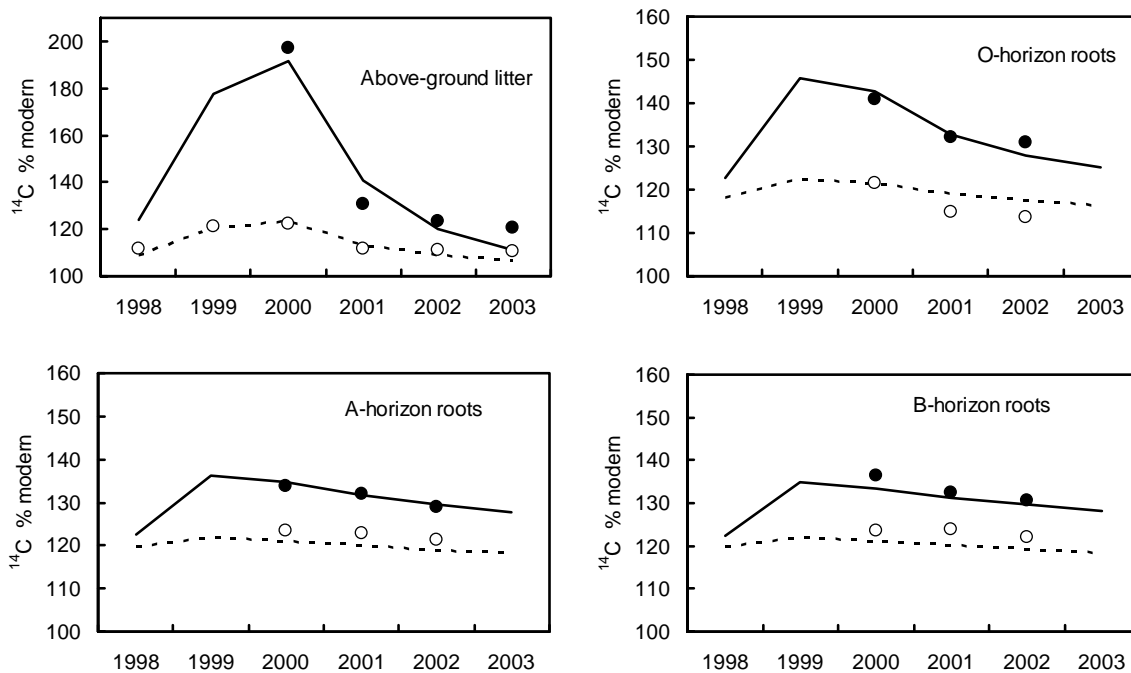


Figure S1 Observed and simulated  $^{14}\text{C}$  contents of above-ground litter and roots. The open symbols and dotted lines refer to east ORR, the closed symbols and full lines to west ORR.

## HYDROLOGY

Interception losses from rainfall were estimated by assuming a maximum loss of 20% during leaf cover (days 100 to 300) and 10% during leaf absence, scaling down to fractional losses of 15 and 7.5 % respectively with increasing rainfall, based on representative observations (Luxmoore and Huff 1989; Ward & Robinson 1990). The average total annual interception loss was forced to 100 mm (Luxmoore and Huff 1989).

The adjustable parameters (Table S2) were found by comparing the model output with (a) the output of the water budget model PROSPER (Huff et al. 1977) parameterised within the stand level model INTRASTAND (Hanson et al. 2004, 2005b), and (b) measured soil moisture contents. The parameters were adjusted to force agreement in total water draining from the A- and B-horizons over the period 2002-2003, and to match as closely as possible the observed soil moisture contents of the A- and B-horizons over the period 2001-2005. The fitting was not very sensitive to the drainage rate constants, but soil moisture depended strongly on the soil macroporosity. Outputs from the optimised model are compared with the target data in Figure S1.

A nonreactive Br tracer was also applied as  $\text{CaBr}_2$  to all soil plots that were used for monitoring for vertical DOC mobility. The application of Br involved a uniform distribution of an aqueous solution to the soil surface via a backpack sprayer as described in Jardine et al. (1990). The intent of the tracer addition was to track the advection and dispersion of pore water movement through the soil profile. Data from the  $\text{CaBr}_2$  tracer experiment were used to assess the model's ability to simulate the passage of a conservative solute through the soil profile and thus track the movement of pore water as a function of time. The tracer was added to the soil surface of four plots at each of the four different sites in December 2001 and concentrations at 15 cm and 70 cm depth were monitored over the subsequent 400 days. The field data from the Haw Ridge and Pine Ridge sites were combined with water fluxes to calculate the average amounts of Br leaving the two horizons over time. We found that the recovery of Br was 65% at 15 cm, and 43% at 70 cm, which we attribute to either lateral transfers or sampler bypass due to preferential advective flow during storm events. These were taken into account by imposing a fractional daily loss (0.04%) of Br. The Br results were used to estimate the solute exchange rate constants ( $D_{\text{exch}}$ ) for the O-, A- and B-horizons, the optimal values being 0.05, 1.0 and 1.0 respectively. Observed and simulated transport of Br are shown in Figure S3.

Table S2 Fitted hydrological parameters by soil horizon.

parameter	horizon	value
evaporation rate constant ( $\text{h}^{-1} \text{ deg}^{-1}$ )	O	$3.2 \times 10^{-5}$
	A	$6.3 \times 10^{-6}$
	B	$4.0 \times 10^{-6}$
drainage rate constant ( $\text{h}^{-1}$ )	A	0.2
	B	0.03
soil macroporosity (unitless)	O	0.50
	A	0.53
	B	0.44

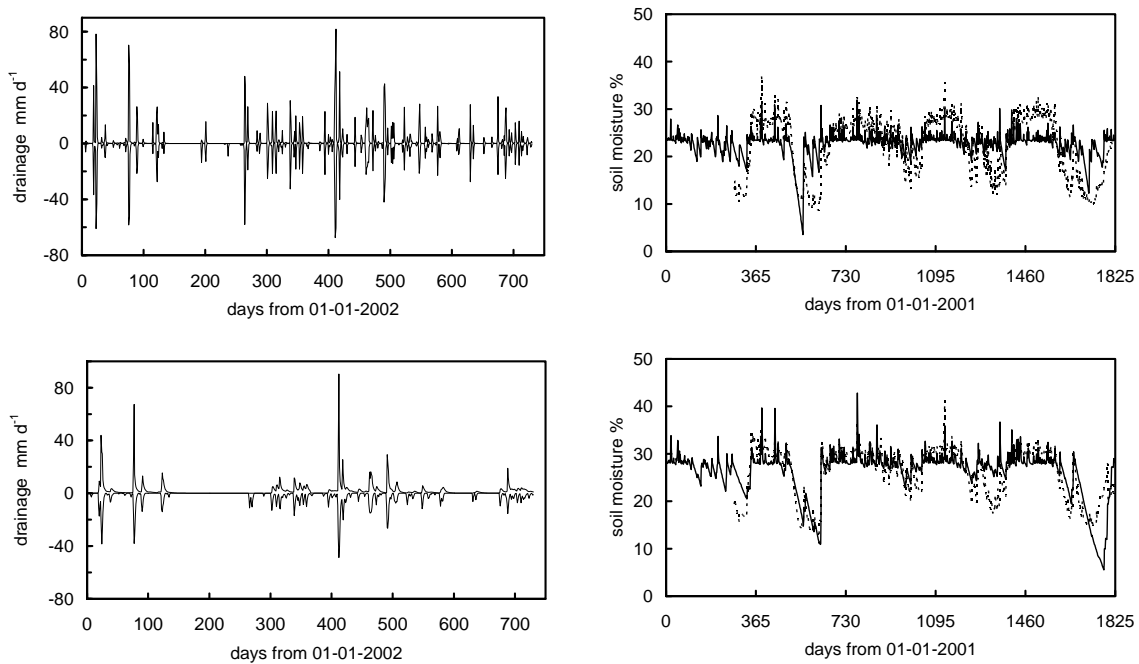


Figure S2 Drainage water and soil moisture. Left plots are the drainage from A (upper) and B (lower) horizons; positive values are from the PROSPER model (Huff et al. 1977) and DyDOC results are shown as negative values to facilitate comparisons. Right, soil moisture in A (upper) and B (lower) horizons where dotted lines are field observations and full lines are the DyDOC simulations.

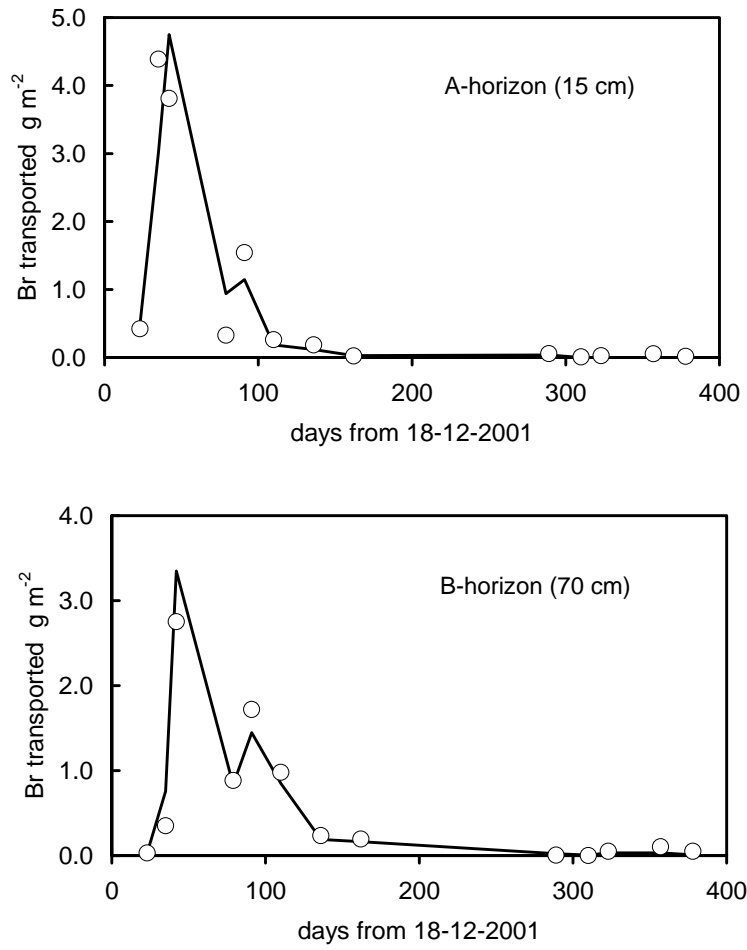


Figure S3 Bromide transport. The points are the means of 16 observations (from 8 samples at each of two sites), and the relative standard deviation is on average 54 % of the mean value. The lines are DyDOC fits.

**OTHER SUPPLEMENTARY FIGURES**

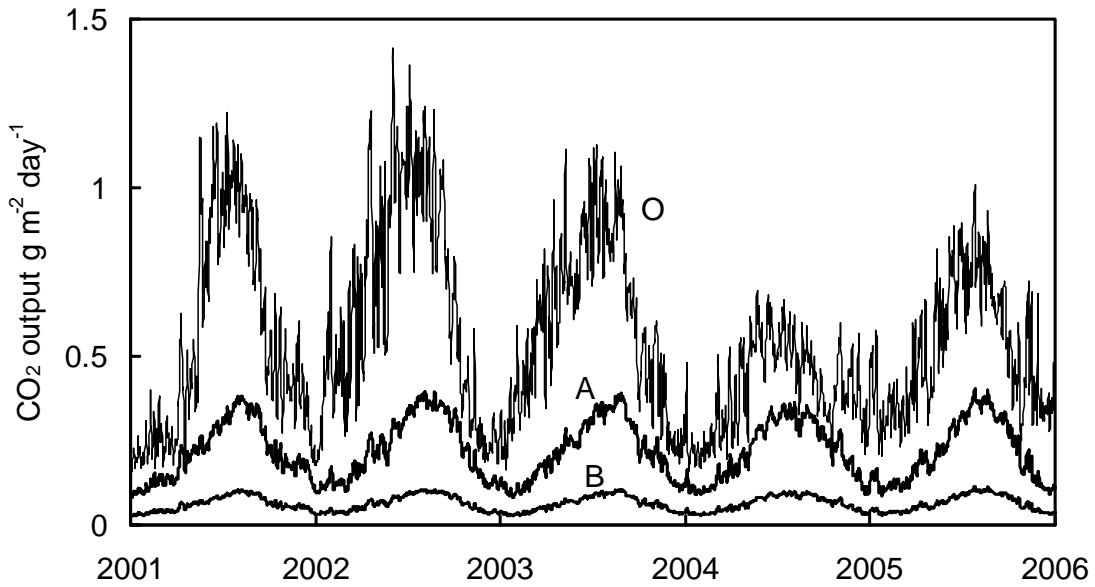


Figure S4 Simulated daily release of CO<sub>2</sub> from the O, A and B horizons.

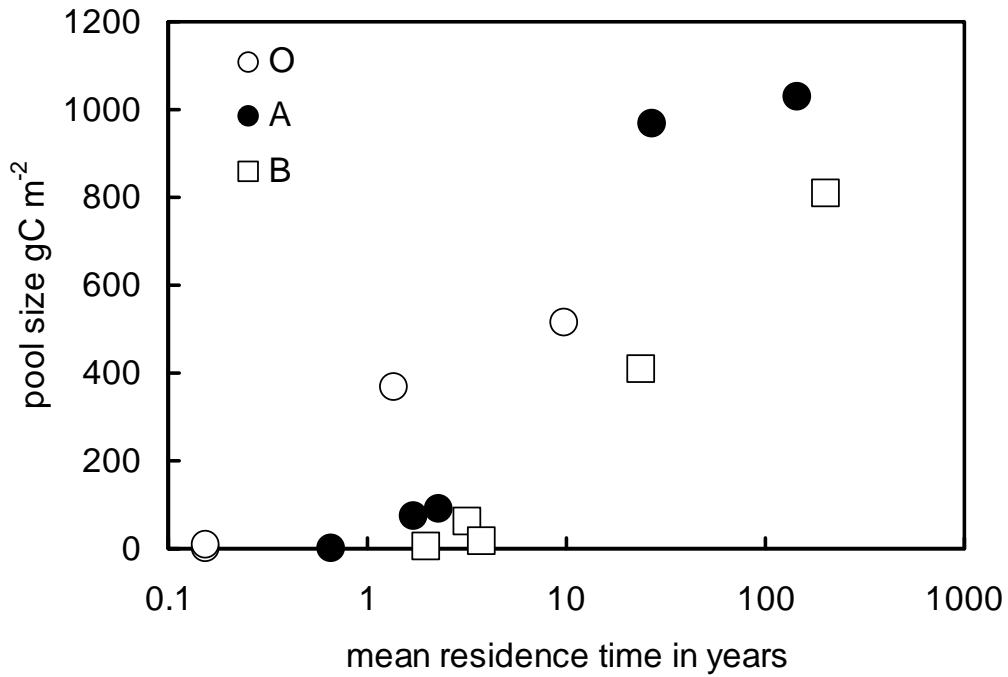


Figure S5 Calculated soil C pools and mean residence times (MRT).

**REFERENCES**

- Dickson R.E. and Larson P.R. 1981. C-14 fixation, metabolic labeling patterns, and translocation profiles during leaf development in *populus-deltoides*. *Planta* 152: 461-470.
- Dickson R.E., Tomlinson P.T., Isebrands J.G. 2000a. Allocation of current photosynthate and changes in tissue dry weight within northern red oak seedlings: individual leaf and flush carbon contribution during episodic growth. *Can. J. For. Res.* 30:1296-1307.
- Dickson R.E., Tomlinson P.T., Isebrands J.G. 2000b. Partitioning of current photosynthate to different chemical fractions in leaves, stems, and roots of northern red oak seedlings during episodic growth. *Can. J. For. Res.* 30:1308-1317
- Gaudinski J.B., Torn M. S., Riley W. J., Swanston C., Trumbore S. E., Joslin J.D., Majdi H., Dawson T.E. and Hanson P. J. 2009. Use of stored carbon reserves in growth of temperate tree roots and leaf buds: analyses using radiocarbon measurements and modelling. *Glob. Change Biol.* 15: 992-1014.
- Hanson P.J., Amthor J.S. Wullschleger S.D., Wilson K.B., Grant R.F., Hartley A., Hui D., Hunt E.R., Johnson D.W., Kimball J.S., King A.W., Luo Y., McNulty S.G., Sun G., Thornton P.E., Wang S., Williams M., Baldocchi D.D. and Cushman R.M. 2004. Oak forest carbon and water simulations: Model intercomparisons and evaluations against independent data. *Ecol. Monogr.* 74: 443-489.
- Hanson P.J., Wullschleger S.D., Norby R.J., Tschaplinski T.J, and Gunderson C.A. 2005b. Importance of changing CO<sub>2</sub>, temperature, precipitation, and ozone on carbon and water cycles of an upland-oak forest: incorporating experimental results into model simulations. *Glob. Change. Biol.* 11: 1402-1423.
- Hua Q. and Barbetti M. 2004. Review of tropospheric bomb <sup>14</sup>C data for carbon cycle modelling and age calibration purposes. *Radiocarbon* 46: 1273–1298.
- Huff D.D., Luxmoore R.J., Mankin J.B. and Begovich C.L. 1977. TEHM: A terrestrial ecosystem hydrology model. ORNL/NSF/EATC-27, Oak Ridge National Laboratory, Oak Ridge, Tennessee.
- Jardine, P.M., G.V. Wilson, and R.J. Luxmoore. 1990. Unsaturated solute transport through a forest soil during rain events. *Geoderma.* 46:103-118.
- Joslin J.D., Gaudinski J.B., Torn M.S., Riley W.J. and Hanson P.J. 2006. Fine-root turnover patterns and their relationship to root diameter and soil depth in a C-14-labelled hardwood forest. *New Phytol.* 172: 523-535.
- Larson P. R. and Gordon J.C. 1969. Leaf development, photosynthesis and <sup>14</sup>C distribution in *Populus deltoides* seedlings. *Am. J. Bot.* 56:1058–1066.



- Levin I. and Kromer B. 2004. The tropospheric  $^{14}\text{CO}_2$  level in mid-latitudes of the Northern Hemisphere (1959-2003). *Radiocarbon* 46: 1261-1272.
- Luxmoore R.J. and Huff D.D. 1989. Water. In Johnson D.W. and Van Hook R.I. *Analysis of Biogeochemical Cycling Processes in Walker Branch Watershed*. Springer, New York.
- Reich P.B., Walters M.B. and Ellsworth D.S. 1991. Leaf age and season influence the relationships between leaf nitrogen, leaf mass per area and photosynthesis in maple and oak trees. *Plant Cell Environ.* 14: 251-259.
- Reimer P.J., Baillie M.G.L., Bard E., Bayliss A., Beck J.W., Bertrand C.J.H., Blackwell P.G., Buck C.E., Burr G.S., Cutler K.B., Damon P.E., Edwards R.L., Fairbanks R.G., Friedrich M., Guilderson T.P., Hogg A.G., Hughen K.A., Kromer B., McCormac G., Manning S., Ramsey C.B., Reimer R.W., Remmele S., Southon J.R., Stuiver M., Talamo S., Taylor F.W., van der Plicht J. and Weyhenmeyer, C.E. 2004. INTCAL04 terrestrial radiocarbon age calibration, 0–26 CAL kyr BP. *Radiocarbon* 46: 1029–1058.
- Ward R.C and Robinson M. 1990. *Principles of Hydrology* (3rd Edition), McGraw-Hill, Maidenhead.